A Switchable Bandpass Filter for Broadband, Dual-Band and Tri-Band Operations

Zizhuo Sun, *Graduate Student Member, IEEE*, Xiaolong Wang, *Member, IEEE* and Kun Li, *Member, IEEE*

***Abstract*— In this letter, a novel microstrip switchable bandpass filter (BPF) is presented. By switching RF p-i-n diodes on/off, the proposed topology could provide three different filtering states: broadband bandpass filter (BBPF), dual-band bandpass filter (DBPF) and tri-band bandpass filter (TBPF). For each state, the relationship between bandwidths and return losses are newly analyzed by proposed algorithm, then the design charts can be easily summarized. In order to improve selectivity and stopband rejection, two cascaded proposed topologies are also considered and discussed briefly. For demonstration, two switchable circuits are designed, fabricated and measured in the experiment. Simulated and measured results are matched very well.**

***Index Terms*—Bandpass filter (BPF), broadband, dual-band, switchable filter, tri-band.**

I. Introduction

MICROWAVE bandpass filter (BPF) [1]-[3] has been widely applied as a basic microwave passive component in modern wireless communication systems. With the rapid development of radio frequency microwave technology, RF components could be able to realize more functionalities within the limited circuit space are in a great demand. Therefore, switchable/multifunctional BPFs have attracted a lot of attentions through using RF p-i-n diodes [1], varactors [4], single-pole double-throw (SPDT) switches [5], liquid metal actuation [6] and so on.

In recent years, increasing the number of switchable/multi -functional BPFs with various circuit topologies have been put forward. For example, a switchable BPF with reconfigurable on-state frequency responses [7] through two switchable delay lines is proposed. Chen and Chu report a dual-band BPF with less tuning elements [8] which could independently control passbands and constant absolute bandwidths, meanwhile, [9]-[10] could also perform similar functionality. Besides dual-band response, [11] implemented by parallel combination of open-circuited and short-circuited stub loaded resonators performs wideband and tri-band operations respectively, however, tri-band bandwidth topologies are quite limited. A series of multi-functional or multi-band reconfigurable BPFs and their analytical synthesis design are presented in [12]-[13], tunable or switchable filtering responses are obtained when the dual-mapping functions are simultaneously controlled to support band-shaping conditions. Furthermore, multi-functional filters are reported with transversal signal-interaction technology [14] or coupled-line structure [15], they could provide both bandpass and bandstop states by turning on/off p-i-n diodes. In [16], by using SPDT switches and varactors, bandpass and bandstop can be switched with controllable bandwidths. Furthermore, a reconfigurable power divider with adjustable phase difference is also considered in [17]. To the best of authors' knowledge, a compact filter with multi-switchable passband has not been reported yet, where multi-passband can be combined by each switchable state with the same bandwidths.

In this letter, a novel microstrip switchable bandpass filter is presented, where three different filtering states: broadband bandpass filter (BBPF), dual-band bandpass filter (DBPF) and tri-band bandpass filter (TBPF) can be easily realized into a single compact component by switching p-i-n diodes on/off. For each state, the relationship between bandwidths and return losses are newly analyzed by proposed algorithm, then the design charts can be easily summarized. In the experiment, two fabricated circuits are selected for verification. Simulated and measured results are matched very well. It is worth mentioning that TBPF can be considered as a combination of BBPF and DBPF approximately. Because the bandwidths and their center frequencies are almost the same when proposed filter is switched from BBPF to TBPF (or from DBPF to TBPF). Such performance is quite useful in wireless communication systems, software-defined radios and electronic warfare support measurement scenarios.

II. Design and Analysis of the Switchable Filter

Fig. 1 shows the symmetrical topology of proposed switchable filter, where all the characteristic impedances with electrical length θ and p-i-n diode switches are labeled in Fig. 1, $\theta = 90^o$@ center frequency f_0. By switching p-i-n diodes on/off, three different filtering states (BBPF, DBPF and TBPF) can be realized into a single topology. To understand the above

Manuscript received Jan. 28, 2022. This work was supported by the National Natural Science Foundation of China (Grant No. 61701189), Project of the Education Department of Jilin Province (Grant No. JJKH20211093KJ), Interdisciplinary Integration and Innovation Project of JLU (Grant No. JLUXKJC2020204), the Project of Science and Technology Development Program of Changchun City (Grant No. 21ZY23) and the Project of Jilin Province Development and Reform Commission (Grant No. 2022C047-6). (*Corresponding author*: Xiaolong Wang)

Zizhuo Sun and Xiaolong Wang are with State Key Laboratory of Integrated Optoelectronics, College of Electronic Science and Engineering, International Center of Future Science, Jilin University, 2699 Qianjin Street, Changchun 130012, China (e-mail: brucewang@jlu.edu.cn).

Kun Li is with the Faculty of Engineering and Design, Kagawa University, Takamatsu 761-0396, Japan (e-mail: li.kun@kagawa-u.ac.jp)

This article has been accepted for publication in IEEE Transactions on Circuits and Systems--II: Express Briefs. This is the author's version which has not been fully edited and content may change prior to final publication. Citation information: DOI 10.1109/TCSII.2022.3203129

filtering states easily, a scheme of general *S*-parameters is shown in Fig. 2. The realizable range of characteristic impedance is defined from 20 Ω to 150 Ω in this letter.

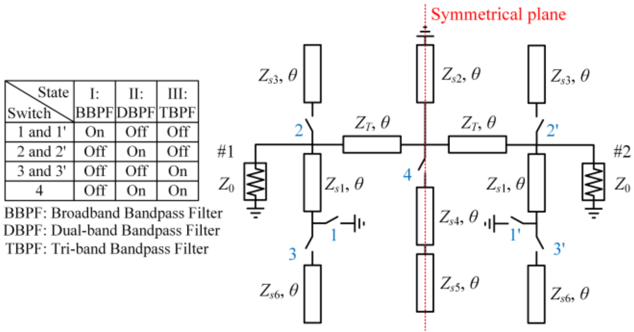

Switch \ State	I: BBPF	II: DBPF	III: TBPF
1 and 1'	On	Off	Off
2 and 2'	Off	On	Off
3 and 3'	Off	Off	On
4	Off	On	On

Fig. 1. The topology of proposed switchable filter.

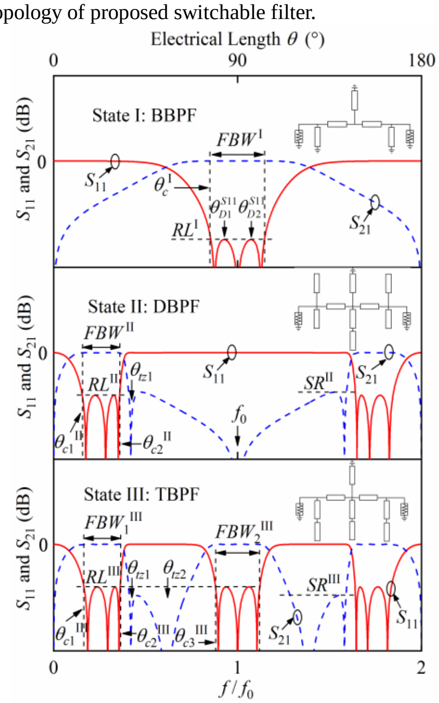

Fig. 2. Corresponding to the three filtering states (BBPF, DBPF and TBPF) of proposed topology in Fig. 1, a scheme of general *S*-parameters.

A. State I: BBPF

From Fig. 1, when the switches 1 and 1' are turned ON and the other switches are turned OFF, the proposed switchable filter becomes a BBPF, which previously appeared in [18]. Due to the existence of three short-circuited stubs, signal cannot be transported from port 1 to 2, thence, $\theta_{tz1} = 0$ or π can be derived when considering the requirement of $|S_{21}| = 0$. According to (1), input impedances of short-circuited stubs are equal to ∞ at center f_0, consequently, the proposed filter shows a bandpass response at state I.

$$Z_{inm} = jZ_{sm}\tan\theta \quad (m = 1, 2) \tag{1}$$

In this letter, the characteristic impedance $Z_T = 70$ Ω and $Z_{s2} = 140$ Ω are selected for facilitate design and analysis. The fractional bandwidth of S_{11} on state I is defined as $FBW^{I} = (1 - \theta_c^{I}) \times 200\%$, where θ_c^{I} represents electrical length at cutoff frequency. By using the synthesis theory in [19], the constraint equations can be summarized: $\partial S_{11}/\partial\theta\big|_{\theta=\theta_{D1}^{S11}\left(or\ \ \theta_{D2}^{S11}\right)} = 0$ and $-20\log_{10}|S_{11}| = RL@\left(\theta_c^{I}, \theta_{D1}^{S11}\right)$. Then, the relationship among FBW^{I}, RL^{I} (return loss of S_{11} on state I) and Z_{s1} can be calculated and shown in Fig. 3. As RL^{I} increases, Z_{s1} is raised, however, FBW^{I} becomes narrower. The realizable range of RL^{I} and FBW^{I} are 15.49 dB < RL^{I} and FBW^{I} < 44.69%, respectively.

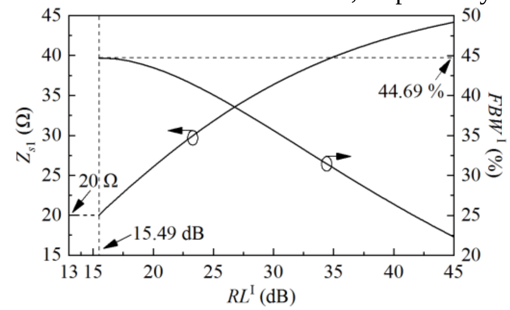

Fig. 3. The relationship among FBW^{I}, RL^{I} and Z_{s1}, which is on the state I under the condition of $Z_T = 70$ Ω and $Z_{s2} = 140$ Ω.

B. State II: DBPF

From Fig. 1, when the switches 2, 4 and 2' are turned ON and the other switches turned OFF, the proposed switchable filter becomes a DBPF. The stepped impedance branch with characteristic impedances Z_{s4} and Z_{s5} is shunted to the middle of circuit topology. Open-circuited stubs (Z_{s1}, θ) are shunted to the input and output ports. Another open-circuited stubs (Z_{s3}, θ) are used to adjust the sum of parallel impedance (Z_{s1} and Z_{s3}). Input impedances of open-circuited stubs are equal to 0 at f_0, which means filter exhibits $|S_{21}| = 0$ at f_0. On the other hand, input impedance of the stepped impedance branch (Z_{in3}) can be derived as

$$Z_{in3} = jZ_{s4}\left(Z_{s4}\tan\theta - Z_{s5}\cot\theta\right)/\left(Z_{s4} + Z_{s5}\right) \tag{2}$$

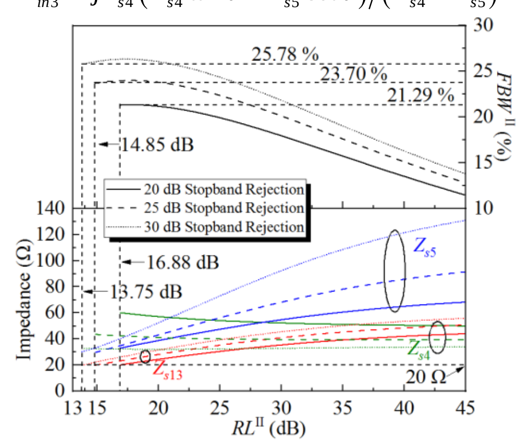

Fig. 4. Relationship among FBW^{II}, RL^{II} and characteristic impedances, which is on the state II under the condition of $Z_T = 70$ Ω and $Z_{s2} = 140$ Ω.

Considering the condition of $Z_{in3} = 0$, $|S_{21}| = 0$ can be obtained and the transmission zeros are calculated as $\theta_{tz1} = \tan^{-1}\sqrt{Z_{s5}/Z_{s4}}$, 90° and $\pi - \theta_{tz1}$, respectively. These three transmission zeros constitute a wide stopband, besides, passband response appears on both sides of the stopband. Therefore, a dual-band bandpass response is established. The fractional bandwidth of S_{11} on state II is defined as $FBW^{II} = (\theta_{c2}^{II} - \theta_{c1}^{II}) \times 100\%$, where, θ_{c1}^{II} and θ_{c2}^{II} represent electrical length at cutoff frequency on state II. The relationship among FBW^{II}, RL^{II} (return loss of S_{11} on state II) and characteristic impedances (Z_{s13}, Z_{s4} and Z_{s5}) is shown in Fig.

This article has been accepted for publication in IEEE Transactions on Circuits and Systems--II: Express Briefs. This is the author's version which has not been fully edited and content may change prior to final publication. Citation information: DOI 10.1109/TCSII.2022.3203129

4, where $Z_{s13} = Z_{s1} // Z_{s3}$. As RL^{II} increases, Z_{s13} and Z_{s5} will be higher, Z_{s4} will be lower, meanwhile, FBW^{II} becomes narrower. Under the condition of 20 dB stopband rejection (*SR*), the realizable range of RL^{II} and FBW^{II} are 16.88 dB < RL^{II} and FBW^{II} < 21.29%, respectively.

C. State III: TBPF

When the switches 3, 4 and 3' are turned ON and the other switches turned OFF, the proposed switchable filter becomes a TBPF. Three stepped impedance branches and a short-circuited stub are all equal to ∞ at f_0, signal can be transported from port 1 to 2. Therefore, bandpass response is achieved around f_0. Under the condition of $|S_{21}| = 0$, the transmission zeros can be similarly derived as $\theta_{tz1} = \tan^{-1}\sqrt{Z_{s5}/Z_{s4}}$, $\theta_{tz2} = \tan^{-1}\sqrt{Z_{s6}/Z_{s1}}$, $\pi - \theta_{tz1}$ and $\pi - \theta_{tz2}$, respectively. These four transmission zeros are dividing a period into three parts, whilst, signal cannot be transported from port 1 to 2 at $\theta = 0$ and π. Hence, TBPF can be achieved. Similarly, the fractional bandwidth of S_{11} on state III is defined as $FBW_1^{\mathrm{III}} = (\theta_{c2}^{\mathrm{III}} - \theta_{c1}^{\mathrm{III}})\times 100\%$ and $FBW_2^{\mathrm{III}} = (1 - \theta_{c3}^{\mathrm{III}})\times 200\%$, where, $\theta_{c1}^{\mathrm{III}}$, $\theta_{c2}^{\mathrm{III}}$ and $\theta_{c3}^{\mathrm{III}}$ stand for electrical length at cutoff frequency on state III.

The relationship among FBW_1^{III}, FBW_2^{III}, RL^{III} (return loss of S_{11} on state III) and characteristic impedances (Z_{s1}, Z_{s4}, Z_{s5} and Z_{s6}) is shown in Fig. 5. As RL^{III} increases, Z_{s1}, Z_{s5} and Z_{s6} will be higher, Z_{s4} will be lower, meanwhile, both FBW_1^{III} and FBW_2^{III} become narrower. Under the condition of SR = 20 dB, the realizable range of RL^{III}, FBW_1^{III} and FBW_2^{III} are 13 dB < RL^{III}, FBW_1^{III} < 18.64 % and FBW_2^{III} < 29.51%, respectively.

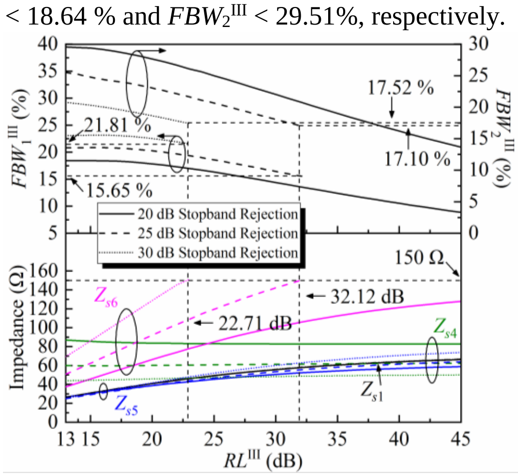

Fig. 5. The relationship among FBW_1^{III}, FBW_2^{III}, RL^{III} and characteristic impedances, which is on the state III under the condition of Z_T = 70 Ω and Z_{s2} = 140 Ω.

D. Flowchart With Algorithm

To demonstrate the design method of proposed switchable filter, its algorithm is summarized as a flowchart in Fig. 6. The brief design steps are described as follows.

Step 1: Specify the desired θ_c, *FBW*, *RL* and *SR* on three states respectively.

Step 2: Based on the above-mentioned specifications, select suitable characteristic impedance Z_T and Z_{s2}.

Step 3: Choose Z_{s1} to match the specifications (θ_c^{I}, FBW^{I} and RL^{I}) of state I. The similar process is reported in Section II. A.

Step 4: Calculate Z_{s13}, Z_{s4} and Z_{s5} to match the specifications ($\theta_{c1}^{\mathrm{II}}$ $\theta_{c2}^{\mathrm{II}}$, FBW^{II}, RL^{II} and SR^{II}) of state II. The similar process is reported in Section II. B. Because Z_{s13} is the parallel of Z_{s1} and Z_{s3}, $Z_{s1} \geqslant Z_{s13}$ must be maintained.

Step 5: Similarly, choose Z_{s6} to match the specifications ($\theta_{c1}^{\mathrm{III}}$ $\theta_{c2}^{\mathrm{III}}$, $\theta_{c3}^{\mathrm{III}}$, FBW_1^{III}, FBW_2^{III}, RL^{III} and SR^{III}) of state III. The similar process is reported in Section II. C. Although all characteristic impedances are determined in this step, they need slight adjustment to fit total specifications for realization.

Step 6: Perform EM simulation and adjust the physical dimensions toward optimized target if necessary.

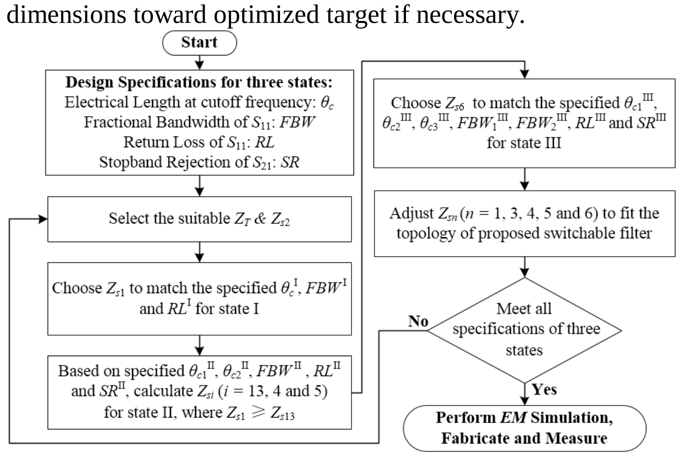

Fig. 6. Design flowchart for the proposed switchable filter.

Furthermore, by cascading multiple proposed switchable filter, equal-ripple numbers can be easily increased with higher selectivity and enhanced *SR*. Fig. 7 shows two cascaded example and its circuit simulation results.

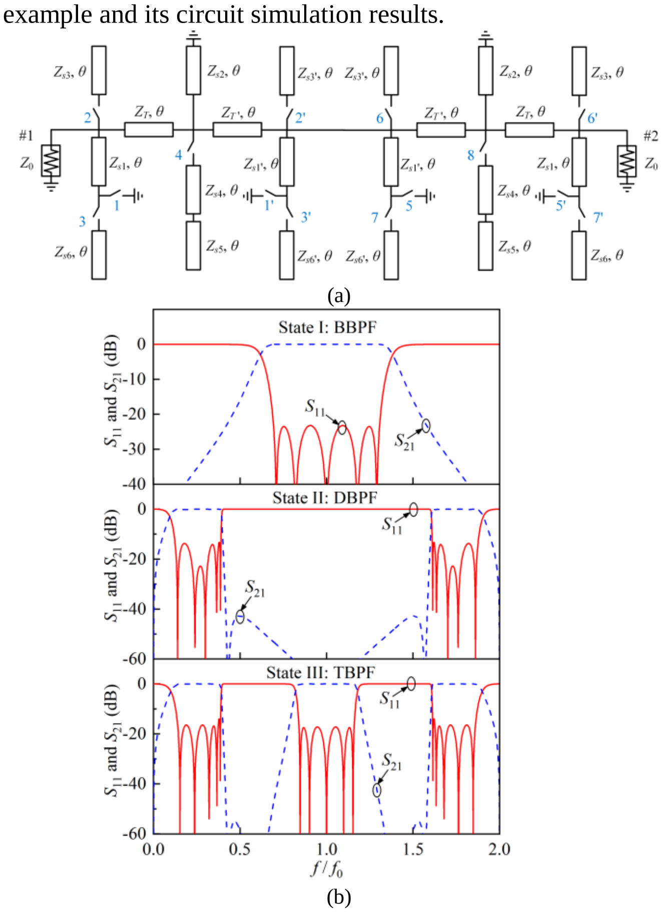

This article has been accepted for publication in IEEE Transactions on Circuits and Systems--II: Express Briefs. This is the author's version which has not been fully edited and content may change prior to final publication. Citation information: DOI 10.1109/TCSII.2022.3203129

Fig. 7. (a) Configuration of the two cascaded switchable filters. (b) Circuit simulation results of cascaded broadband state (switches 1, 1' and 5, 5' are at ON states), cascaded dual-band state (switches 2, 2' and 6, 6' and 4 and 8 are at ON states) and Circuit simulation results of cascaded tri-band state (switches 3, 3' and 7, 7' and 4 and 8 are at ON states). The parameters are Z_T = 64.7 Ω, $Z_{T'}$ = 63.9 Ω, Z_{s1} = 42.8 Ω, $Z_{s1'}$ = 44.8 Ω, Z_{s2} = 181 Ω, Z_{s3} = 50.3 Ω, $Z_{s3'}$ = 40.3 Ω, Z_{s4} = 60.7 Ω, Z_{s5} = 39 Ω, Z_{s6} = 82.6 Ω, $Z_{s6'}$ = 76.5 Ω.

III. Fabrication and Experiment

To experimentally validate the proposed switchable filter concept, two filters are designed, fabricated, and measured, respectively. The parameters of the Rogers RT 5880 substrate are ε_r = 2.2, tanδ = 0.0009, h = 0.787 mm, and t = 0.0175 mm.

For the first filter, the design parameters are Z_T = 70 Ω, Z_{s1} = 40.9 Ω, Z_{s2} = 140 Ω, Z_{s3} = 54.4 Ω, Z_{s4} = 64.2 Ω, Z_{s5} = 38.5 Ω and Z_{s6} = 85.5 Ω under the condition of FBW^{I} = 29.2%, FBW^{II} = 20.4%, FBW_1^{III} = 20.0% and FBW_2^{III} = 25.2%. From the measured results, we could easily find that: (1) When the proposed filter is switched from BBPF to TBPF, the bandwidth of the center frequency is almost the same, where $FBW^{I} \approx FBW_2^{III}$. (2) Similarly, when the proposed filter is switched from DBPF to TBPF, the bandwidth of the dual-frequency is almost the same, where $FBW^{II} \approx FBW_1^{III}$. Therefore, TBPF can be considered as a combination of BBPF and DBPF approximately, and the above performance is quite useful for wireless communication systems application. The layout and photograph of fabricated circuit are shown in Fig. 8 (a), where, the capacitors and the resistors applied in the biasing networks of the RF p-i-n diodes are C_{bia} = 1000 pF and R_{bia} = 10 kΩ respectively. RF p-i-n diodes SMP1345-079LF from Skyworks were used for switching three states. The EM simulated and measured results are shown in Fig. 8 (b), and they are matched very well. For the second filter, the design parameters are listed in Fig. 7. The photograph of fabricated circuit is shown in Fig. 9 (a), and its EM simulated and measured results are shown in Fig. 9 (b).

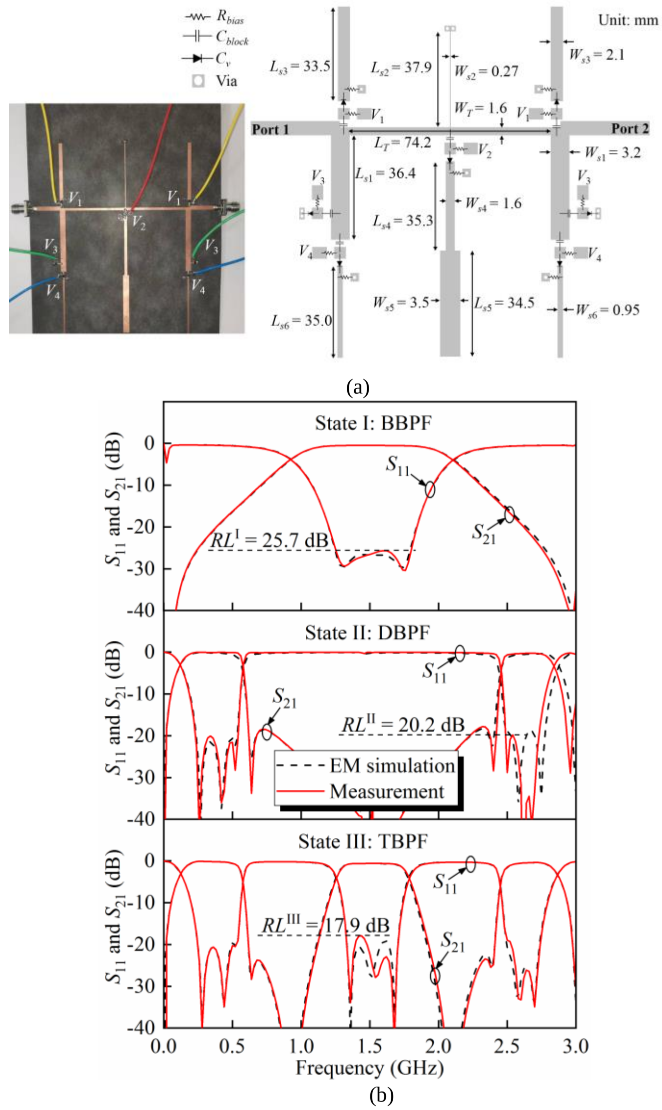

Fig. 8. The first experimental switchable filter. (a) The layout and photograph of proposed work. (b) The EM simulation and measurement.

TABLE I
Comparisons With Recent Switchable/Multifunctional Filters

Reference	Responses	Fractional bandwidth (%)	Return loss (dB)	In-band insertion loss (dB)	Number of diodes	Circuit size ($\lambda_g \times \lambda_g$)	Excellent multi-band switching configuration
[11]	BBPF / TBPF	102 / 11.6 & 4.2 & 6.7	>10 / >10	<1.7 / <1.7	10	0.71×0.45	No
[13]	BBPF / DBPF	34# / 16.7 & 13.0#	- / -	<0.5 / <0.6	9	0.80×0.60	No
	BPF / DBPF / TBPF / QBPF	7.5# / 5.5 & 6.0# / 3.5 & 5.9 & 1.8# / 3.4 & 3.0 & 2.7 & 2.2#	- / - / - / -	<1.6 / <3.2 / <3.2 / <3.0	16	1.15×0.88	No
[14]	BBPF / BPF / BSF	95.7 / 25.3 / 106	>11.4 / >15 / -	<0.9 / <0.8 / <15.0	6	0.50×0.25	No
[15]	BBPF / BSP / DBPF	53.1 / 30.2 / 3.8 & 2.7	>10 / - / >10	<0.9 / <15.5 / <2.2	6	0.44×0.29	No
[16]	BBPF / BSF	55.6 / 12.6	>15 / -	<3.0 / <15.0	4	0.80×0.45	No
	DBPF / DBSF	14.0 & 8.5 / 13.2 & 3.6	>15 / -	<4.7 / <15.0	7	0.84×0.55	No
This work	**BBPF / DBPF / TBPF**	**36.7 / 20.7 & 16.1 / 20.0 & 27.4 & 18.1**	**>25.7 / >20.2 / >17.9**	**<0.5 / <0.4 / <0.6**	**7**	**0.75×0.40**	**Yes**

QBPF: Quad-band Bandpass Filter, #: 3-dB *FBW*.

This article has been accepted for publication in IEEE Transactions on Circuits and Systems--II: Express Briefs. This is the author's version which has not been fully edited and content may change prior to final publication. Citation information: DOI 10.1109/TCSII.2022.3203129

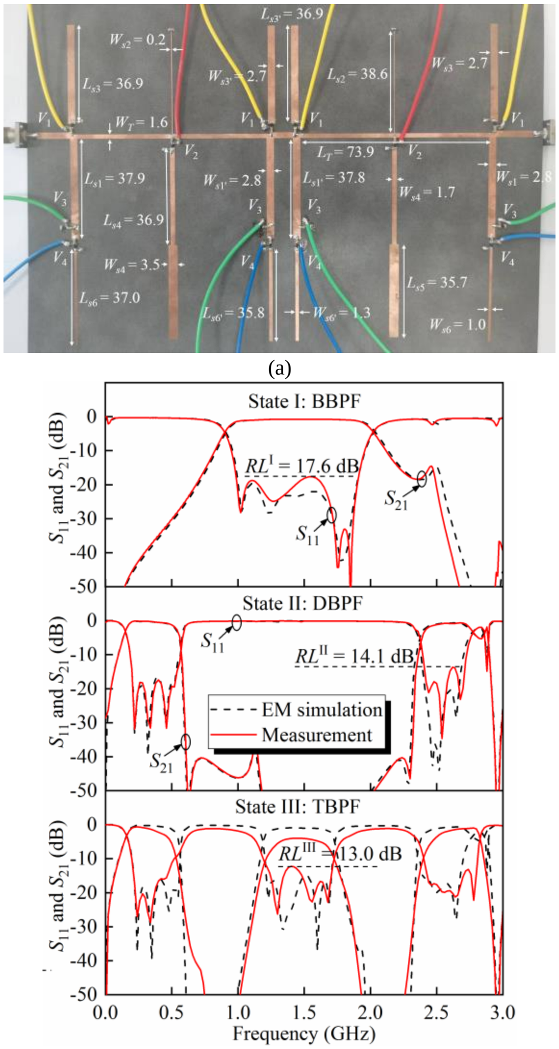

Fig. 9. The second experimental switchable filter. (a) The photograph of proposed work. (b) The EM simulation and measurement.

Comparing with former switchable/multifunctional filters, the advantages of proposed work are listed in Table I. The main improvements are listed as follows: (1) The proposed work provides BBPF, DBPF and TBPF into a single component, where, TBPF can be considered as a combination of BBPF and DBPF approximately. (2) Based on the design charts of three states, different bandwidths and return losses can be controlled for the proposed filter. (3) Three different states can be realized with less diodes and compact size and better performance.

IV. Conclusion

A novel switchable filter with three different states is proposed in this letter. The proposed filter with compact size simple circuit topology structure provides an excellent innovation for multi-band application scenarios in wireless communication systems, software-defined radios and electronic warfare support measurement scenarios.

References

[1] A. Miller and J. S. Hong, "Wideband bandpass filter with reconfigurable bandwidth,'' *IEEE Microw. Wireless Compon. Lett.*, vol. 20, no. 1, pp. 28–30, Jan. 2010.

[2] K. -D. Xu, S. Lu, Y. Guo, and Q. Chen, "Quasi-reflectionless filters using simple coupled line and T-shaped microstrip structures," *IEEE Journal of Radio Frequency Identification*, vol. 6, no. 1, pp. 54-63, Dec. 2022.

[3] K. -D. Xu, S. Xia, Y. Jiang, Y Guo, Y. Liu, R. Wu, J. Cui, and Q Chen, "Compact millimeter-wave on-chip dual-band bandpass filter in 0.15-μm GaAs Technology," *IEEE Journal of the Electron Devices Society*, vol. 10, pp. 152-156, Feb. 2022.

[4] H.-J. Tsai, B.-C. Huang, N.-W. Chen, and S.-K. Jeng, "A reconfigurable bandpass filter based on a varactor-perturbed, T-shaped dual-mode resonator," *IEEE Microw. Wireless Compon. Lett.*, vol. 24, no. 5, pp. 297–299, May. 2014.

[5] T.-H. Lee, J.-J. Laurin, and K. Wu, "Reconfigurable filter for bandpass-to-absorptive bandstop responses," *IEEE Access*, vol. 8, pp. 6484–6495, 2020.

[6] S. N. Mcclung, S. Saeedi, and H. H. Sigmarsson, "Band-reconfigurable filter with liquid metal actuation," *IEEE Trans. Microw. Theory Techn.*, vol. 66, no. 6, pp. 3073–3080, Jun. 2018.

[7] W. H. Tu, "Switchable microstrip bandpass filters with reconfigurable on-state frequency responses," *IEEE Microw. Wireless Compon. Lett.*, vol. 20, no. 5, pp. 259–261, May. 2010.

[8] Z. H. Chen and Q. X. Chu, "Dual-band reconfigurable bandpass filter with independently controlled passbands and constant absolute bandwidths," *IEEE Microw. Wireless Compon. Lett.*, vol. 26, no. 2, pp. 92–94, Feb. 2016.

[9] X.-K. Bi, X. Zhang, W.-S. Wong, T. Yuan, and S.-H. Guo, "Synthesis design of Chebyshev wideband bandpass filters with independently reconfigurable lower passband edge," *IEEE Trans. Circuits Syst. II, Exp. Briefs.*, vol. 67, no. 12, pp. 2948–2952, Dec. 2020.

[10] M. Fan, K. Song, and Y. Fan, "Reconfigurable bandpass filter with wide-range bandwidth and frequency control," *IEEE Trans. Circuits Syst. II, Exp. Briefs.*, vol. 68, no. 6, pp. 1758–1762, Jun. 2021.

[11] A. Bandyopadhyay, P. Sarkar, T. Mondal and R. Ghatak, "A dual function reconfigurable bandpass filter for wideband and tri-Band operations," *IEEE Trans. Circuits Syst. II, Exp. Briefs.*, vol. 68, no. 6, pp. 1892–1896, June. 2021.

[12] R. Zhang, R. Gomez-Garcia, and D. Peroulis, ''Multifunctional bandpass filters with reconfigurable and switchable band control,'' *IEEE Trans. Microw. Theory Techn.*, vol. 67, no. 6, pp. 2355–2369, Jun. 2019.

[13] R. Gómez-García, and A. C. Guyette, "Reconfigurable multi-band microwave filters," *IEEE Trans. Microw. Theory Techn.*, vol. 63, no. 4, pp. 1294–1307, Apr. 2015.

[14] W. Feng, Y. Shang, W. Che, R. Gómez-García, and Q. Xue, "Multifunctional reconfigurable filter using transversal signal-interaction concepts," *IEEE Microw. Wireless Compon. Lett.*, vol. 27, no. 11, pp. 980–982, Nov. 2017.

[15] D. Li and K. -D. Xu, "Multifunctional switchable filter using coupled-line structure," *IEEE Microw. Wireless Compon. Lett.*, vol. 31, no. 5, pp. 457-460, May. 2021.

[16] N. Kumar and Y. K. Singh, "RF-MEMS-based bandpass-to-bandstop switchable single- and dual-band filters with variable FBW and reconfigurable selectivity," *IEEE Trans. Microw. Theory Techn.*, vol. 65, no. 10, pp. 3824–3837, Oct. 2017.

[17] L. Guo, H. Zhu, and A. Abbosh, "Phase reconfigurable microwave power divider," *IEEE Trans. Circuits Syst. II, Exp. Briefs.*, vol. 66, no. 1, pp. 21–25, Jan. 2019.

[18] L. Zhu, S. Sun, and R. Li, *Microwave Bandpass Filters for Wideband Communications*. New York, NY, USA: Wiley, 2012.

[19] N. Zhang, X. Wang, L. Zhu and G. Lu, "A Wideband Bandpass Power Divider With Out-of-Band Multi-Transmission Zeros and Controllable Equal-Ripple Levels," *IEEE Trans. Microw. Theory Techn.*, vol. 70, no. 2, pp. 1178-1187, Feb. 2022.